Available online at www.sciencedirect.com
SCIENCE DIRECT®
Journal of Sound and Vibration 282 (2005) 231–248
JOURNAL OF SOUND AND VIBRATION
www.elsevier.com/locate/jsvi

The effect of stacking sequence and coupling mechanisms on the natural frequencies of composite shafts

H.B.H. Gubran[a,*], K. Gupta[b]

[a]*Mechanical Engineering Department, Faculty of Engineering, University of Aden, P.O. Box 5243, Aden, Yemen*
[b]*Mechanical Engineering Department, Indian Institute of Technology, Delhi, India*

Received 15 January 2002; received in revised form 12 February 2004; accepted 18 February 2004
Available online 25 September 2004

Abstract

In this paper the natural frequencies of composite tubular shafts have been analysed. Equivalent modulus beam theory (EMBT) with shear deformation, rotary inertia and gyroscopic effects has been modified and used for the analysis. The modifications take into account effects of stacking sequence and different coupling mechanisms present in composite materials. Results obtained have been compared with that available in the literature using different modelling. The close agreement in the results obtained clearly show that, in spite of its simplicity, modified EMBT can be used effectively for rotordynamic analysis of tubular composite shafts.

1. Introduction

Several investigators [1–4] have used beam formulation in the analysis of composite shafts. In this approach, the shaft is represented as a beam of a circular cross-section. Singh and Gupta [5] have shown that equivalent modulus beam theory (EMBT) can be used effectively for the analysis of tubular composite shafts of symmetric configurations and can be easily extended for rotordynamic analysis. However, their analysis has shown that formulation based on EMBT has some limitations for unsymmetric configurations because of which it may lead to inaccurate

*Corresponding author.
E-mail address: h_gubran@yahoo.com (H.B.H. Gubran).

0022-460X/$ - see front matter © 2004 Elsevier Ltd. All rights reserved.
doi:10.1016/j.jsv.2004.02.022

predictions of rotordynamic behaviour. Cheng and Peng [6,7] used finite element model based on Timoshenko beam theory to obtain the matrix equation of motion for rotating shafts.

In the present analysis several refinements have been made in EMBT to account for unsymmetric configuration, plies stacking sequence and different coupling mechanisms effect. The layerwise beam theory (LBT) has been refined to account for shear normal coupling effect. Results obtained from both theories have been compared [5].

2. Formulation based on beam theory

The limitations of the existing EMBT have been presented. Refinements made in EMBT are then presented. Later shear normal coupling effect has been incorporated in LBT.

2.1. Equivalent modulus beam theory (EMBT)

In EMBT, the equivalent longitudinal and inplane shear modulii are determined using Classical Laminate Theory (CLT). These modulii are used to calculate shaft natural frequencies using Timoshenko beam theory in the same manner as that for isotropic shafts. In spite of its simplicity and good results obtained for balanced symmetric configuration, several limitations have been pointed out and they are summarized below.

(i) In multilayered composite shaft, different layers (plies) have different contributions to the overall stiffness of the shaft depending on their locations from the mid-plane. However, EMBT does not account for the locations of the individual plies and accordingly the equivalent longitudinal and inplane shear modulii are independent of the stacking sequence of a particular configuration.
(ii) For unbalanced configuration, shear–normal and bending–twisting couplings are present. These couplings affect significantly shaft natural frequencies. However, these effects are not incorporated in EMBT formulation.
(iii) In unsymmetric configurations, bending–stretching coupling is present which affects the shaft natural frequencies. This effect is also not included in the EMBT formulation.

2.2. Modified equivalent modulus beam theory

A Bresse–Timoshenko beam with transverse shear deformation, rotary inertia and gyroscopic effects included is considered. The theory is generalized to include bending–twisting, shear–normal and bending–stretching coupling effects. To account for the locations of different plies and their stacking sequence, longitudinal and inplane shear modulii are taken in the ply level.

2.2.1. Assumptions

The following are the main assumptions adopted for the analysis of shaft natural frequency using beam theory:

(i) The cross-section of the shaft is circular,
(ii) No axial forces and torque on the shaft and,
(iii) All nonlinearities and higher order terms are neglected.

2.2.2. Formulation

Consider a simply supported shaft as shown in Fig. 1a and b. The displacement field is described by the transverse displacements, w and v measured in the z and y directions, the bending slopes α and β in the x–z and x–y planes and φ is the shaft twist angle. The quantities w, v, α, β and φ are assumed to be time dependent and are expressed as

$$w = \bar{w}e^{i\Omega t}, \quad v = \bar{v}e^{i\Omega t}, \quad \alpha = \bar{\alpha}e^{i\Omega t}, \quad \beta = \bar{\beta}e^{i\Omega t}, \quad \phi = \bar{\phi}e^{i\Omega t}, \tag{1}$$

where Ω is the whirl frequency.

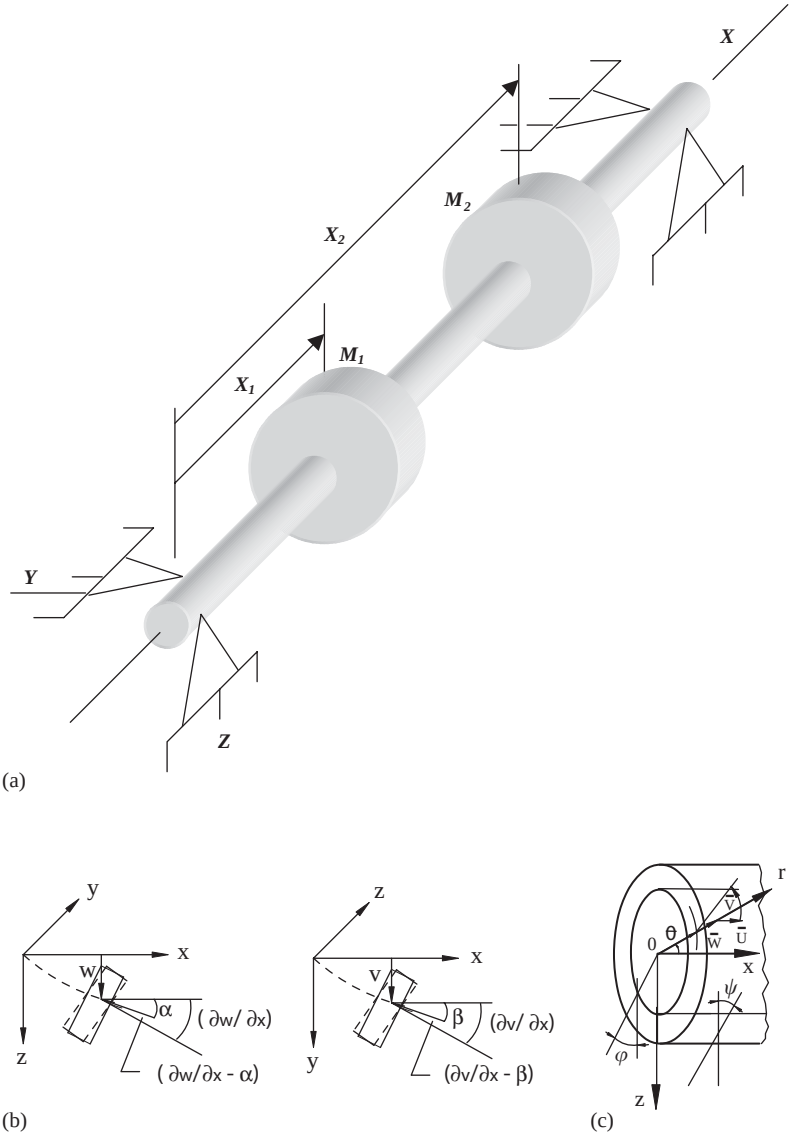

Fig. 1. (a) Coordinate system of the rotor, (b) Cartesian and (c) cylindrical.

The strain energy of the shaft including bending in two planes, shear deformation and torsional energy can be expressed [8] as

$$U = \frac{1}{2}\int_0^l \left\{ C_B\left[\left(\frac{\partial\alpha}{\partial x}\right)^2 + \left(\frac{\partial\beta}{\partial x}\right)^2\right] + C_S\left[\left(\frac{\partial w}{\partial x} - \alpha\right)^2 + \left(\frac{\partial v}{\partial x} - \beta\right)^2\right] + C_T\left(\frac{\partial\phi}{\partial x}\right)^2 \right\} \mathrm{d}x, \quad (2)$$

where C_B is the bending stiffness coefficient which can be given [3] by

$$C_B = \frac{\pi}{4}\sum_{k=1}^{n} \bar{Q}_{11}^{(k)}\left[r_{o(k)}^4 - r_{i(k)}^4\right]. \quad (3)$$

The torsional stiffness coefficient C_T [3] is

$$C_T = \frac{\pi}{2}\sum_{k=1}^{n} \bar{Q}_{66}^{(k)}\left[r_{o(k)}^4 - r_{i(k)}^4\right] \quad (4)$$

and the shear stiffness coefficient C_S is given by

$$C_S = k' A G_{X\theta}, \quad (5)$$

where k' is the shear correction factor which can be taken, for thin tubes, as $\frac{1}{2}$.

In Eqs. (3) and (4), $r_o^k, r_i^k, \bar{Q}_{11}^{(k)}$ and $\bar{Q}_{66}^{(k)}$ are the outer radii, inner radii, longitudinal and shear stiffness coefficients of the kth ply, respectively.

The total kinetic energy is the sum of the kinetic energies the shaft and the discs mounted on it. This can be expressed [8] as

$$T = \frac{1}{2}\int_0^l \left[\rho A(\dot{w}^2 + \dot{v}^2) + \rho I(\dot{\alpha}^2 + \dot{\beta}^2) + \rho I_p\dot{\phi}^2 + 2\rho I_p\omega\dot{\alpha}\beta\right] \mathrm{d}x$$
$$+ \frac{1}{2}\sum_{i=1}^{ND}\left[M_{Di}(\dot{w}(x_i)^2 + \dot{v}(x_i)^2) + I_{DTi}(\dot{\alpha}(x_i)^2 + \dot{\beta}(x_i)^2) + 2I_{DPi}\omega\dot{\alpha}(x_i)\beta(x_i)\right]. \quad (6)$$

Here ρ is the mass density of the shaft material, A, I and I_p are area, lateral and polar area moments of inertia of the shaft cross-section. M_{Di}, I_{DTi} and I_{DPi} are mass, lateral and polar mass moments of inertia of the ith disc, respectively. The rotational angular speed of the shaft is ω. The first, second, third and fourth set of terms within the integral sign give the effect of translatory, rotary and torsional inertia, and gyroscopic moment of the shaft. The four terms within the summation sign give the same effects for the discs mounted on the shaft.

2.2.3. Solution equations

The series solution functions are assumed for w, v, α, β and ϕ in the form

$$\bar{w}(x) = \sum_{j=1}^{n} W_j \sin\frac{j\pi x}{l}, \quad \bar{v}(x) = \sum_{j=1}^{n} V_j \sin\frac{j\pi x}{l},$$
$$\bar{\alpha}(x) = \sum_{j=1}^{n} A_j \cos\frac{j\pi x}{l}, \quad \bar{\beta}(x) = \sum_{j=1}^{n} B_j \cos\frac{j\pi x}{l},$$

$$\bar{\phi}(x) = \sum_{j=1}^{n} \Phi_j \cos\frac{j\pi x}{l}. \tag{7}$$

Here n is the total number of terms in the series solutions. The above functions satisfy geometric boundary conditions at $x = 0$ and $x = l$. The Lagrangian $L = U - T$ is set up from strain and kinetic energies and made stationary with respect to the solution coefficients, i.e.

$$\frac{\partial L}{\partial W_j} = 0, \quad \frac{\partial L}{\partial V_j} = 0, \quad \frac{\partial L}{\partial A_j} = 0, \quad \frac{\partial L}{\partial B_j} = 0, \quad \frac{\partial L}{\partial \Phi_j} = 0. \tag{8}$$

The time dependence cancels out in all the terms and a set of $5n$ simultaneous algebraic equations in the form of a quadratic eigenvalue problem is obtained as

$$\left[-\Omega^2[M] + \mathrm{i}\Omega[D] + [K]\right]\{X\} = \{0\}. \tag{9}$$

Here the matrix $[D]$ involves the contribution due to the gyroscopic effect and is dependent on rotational speed. The eigenvector $\{X\}$ is given by

$$\{X\} = [W_1, W_2, \ldots, W_n \quad V_1, V_2, \ldots, V_n \quad A_1, A_2, \ldots, A_n \quad B_1, B_2, \ldots, B_n \quad \Phi_1, \Phi_2, \ldots, \Phi_n]^{\mathrm{T}}. \tag{10}$$

2.3. Improvement to include different coupling mechanisms

Several refinements have been made to account for different coupling mechanisms effects, namely, Poisson's effect, shear–normal and bending–twisting coupling effects. Generally, the strain energy in the shaft is given by

$$U = \sum_{k=1}^{n} U^k = \frac{1}{2}\sum_{k=1}^{n} \int_v [\sigma^k]\{\varepsilon^k\}\,\mathrm{d}v. \tag{11}$$

The summation is taken over all the plies contained in the laminate, and

$$[\sigma]^k = \begin{Bmatrix} \sigma_{xx} \\ \sigma_{\theta\theta} \\ \tau_{x\theta} \end{Bmatrix}^k = \begin{bmatrix} \bar{Q}_{11} & \bar{Q}_{12} & \bar{Q}_{16} \\ \bar{Q}_{12} & \bar{Q}_{22} & \bar{Q}_{26} \\ \bar{Q}_{16} & \bar{Q}_{26} & \bar{Q}_{66} \end{bmatrix}^k \begin{Bmatrix} \varepsilon_{xx} \\ \varepsilon_{\theta\theta} \\ \varepsilon_{x\theta} \end{Bmatrix}^k. \tag{12}$$

Here σ_{xx} and $\sigma_{\theta\theta}$ are inplane normal and hoop stresses and $\tau_{x\theta}$ is the inplane shear stress, ε_{xx} and $\varepsilon_{\theta\theta}$ are the inplane normal and hoop strains and $\varepsilon_{x\theta}$ is the inplane shear strain in x and θ coordinates as shown in Fig. 1c. $[\bar{Q}]$ is the transformed stiffness matrix of the kth ply.

2.3.1. Improvement to include Poisson's coupling effect

In a thin single ply, shear effect is negligible and bending–stretching and shear–normal coupling effects are not present. However, in calculating strain energy, ε_θ is taken to be zero, which implies some effective stress occurs in θ-direction. But in the actual case no such stress acts. Thus, imposition of the condition of no cross-section deformation results in no strain condition in the circumferential direction and this gives higher frequency values. The circumferential stress in each

ply is assumed to be zero, thus from Eq. (12),

$$\sigma_{\theta\theta}^{(k)} = \bar{Q}_{22}^{(k)}\varepsilon_{\theta\theta}^{(k)} + \bar{Q}_{12}^{(k)}\varepsilon_{xx}^{(k)} = 0.$$

This gives

$$\varepsilon_{\theta\theta}^{(k)} = -\frac{\bar{Q}_{12}^{(k)}\varepsilon_{xx}^{(k)}}{\bar{Q}_{22}^{(k)}}.$$

Also from Eq. (12) we have

$$\sigma_{xx}^{(k)} = \bar{Q}_{11}^{(k)}\varepsilon_{xx}^{(k)} + \bar{Q}_{12}^{(k)}\varepsilon_{\theta\theta}^{(k)}.$$

Substituting for $\varepsilon_{\theta\theta}^{(k)}$ from above

$$\sigma_{xx}^{(k)} = \left(\bar{Q}_{11}^{(k)} - (\bar{Q}_{12}^{(k)})^2/\bar{Q}_{22}^{(k)}\right)\varepsilon_{xx}^{(k)} = \bar{Q}_{11m}^{(k)}\varepsilon_{xx}^{(k)}, \tag{13a}$$

where

$$\bar{Q}_{11m}^{(k)} = \left(\bar{Q}_{11}^{(k)} - (\bar{Q}_{12}^{(k)})^2/\bar{Q}_{22}^{(k)}\right). \tag{13b}$$

Thus the value of $\bar{Q}_{11}$ is updated to account for Poisson's effect according to Eq. (13b).

2.3.2. Improvement to include shear–normal coupling effect

In conventional filament winding procedure the fibres at winding angles $\pm\theta$ are interwoven in the same ply; similarly for configurations in which corresponding to $+\theta$ orientation ply above the mid-plane, there is an identical ply (material and thickness) of $-\theta$ orientation below the mid-plane as shown in Fig. 2a; the shear–normal coupling effect is eliminated. However, if the shaft is made from prepregs to provide a single winding angle, then shear–normal coupling (due to the terms $\bar{Q}_{16} \neq 0$ and $\bar{Q}_{26} \neq 0$) will be present. Generally, coupling exists between normal stress (σ_{xx}) with shear strain ($\varepsilon_{x\theta}$) and shear stress ($\tau_{x\theta}$) with normal strain (ε_{xx}). From the classical laminate theory, the forces on the laminate are related with strain as follows

$$\{N\} = [A_{ij}]\{\varepsilon\} \tag{14}$$

or

$$\{\varepsilon\} = [A_{ij}]^{-1}\{N\}. \tag{15}$$

For a uniaxial load in longitudinal direction and laminate of total thickness t, $N_{xx} = t\sigma_{xx}$, $N_{\theta\theta} = 0$, and $N_{x\theta} = 0$. Then

$$\varepsilon_{xx} = \frac{a\sigma_{xx}t}{\Delta} \quad \text{or} \quad \frac{\sigma_{xx}}{\varepsilon_{xx}} = E_{xx} = \frac{\Delta}{at},$$

where $\Delta = A_{11}a - A_{12}b + A_{16}c$ and a, b and c are the cofactors of A_{11}, A_{12} and A_{16}, respectively given by

$$a = A_{22}A_{66} - A_{26}^2 \quad \text{for single ply } k, \quad a^k = \bar{Q}_{22}^k\bar{Q}_{66}^k - (\bar{Q}_{26}^k)^2,$$

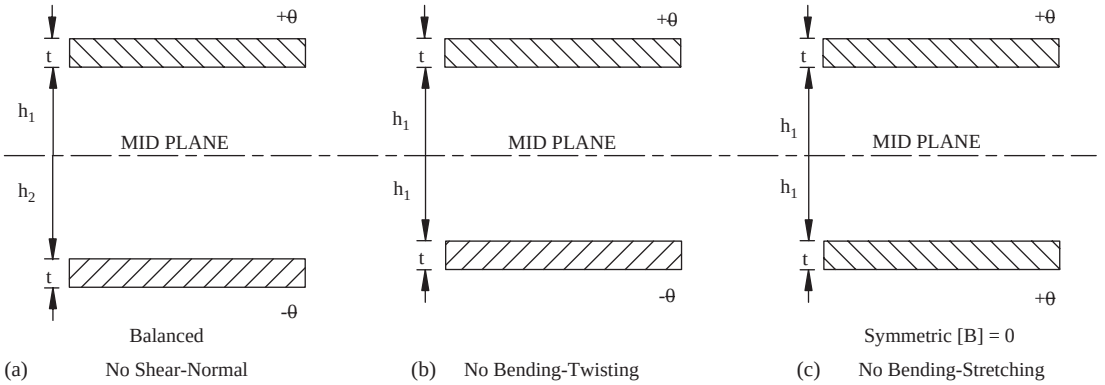

Fig. 2. (a) Shear–normal coupling, (b) bending–twisting coupling, and (c) bending–stretching coupling.

$$b = A_{12}A_{66} - A_{16}A_{26} \quad \text{for single ply } k, \quad b^k = \bar{Q}^k_{12}\bar{Q}^k_{66} - \bar{Q}^k_{16}\bar{Q}^k_{26},$$
$$c = A_{12}A_{26} - A_{16}A_{22} \quad \text{for single ply } k, \quad c^k = \bar{Q}^k_{12}\bar{Q}^k_{26} - \bar{Q}^k_{16}\bar{Q}^k_{22}.$$

The longitudinal and shear modulii can be given by

$$E_{xx} = \frac{\sigma_{xx}}{\varepsilon_{xx}} = (A_{11}a - A_{12}b + A_{16}c)/(at). \tag{16a}$$

Similarly, applying $N_{x\theta}$ and keeping $N_{xx} = N_{\theta\theta} = 0$, one obtains

$$G_{x\theta} = \frac{\tau_{xy}}{\varepsilon_{xy}} = (A_{11}a - A_{12}b + A_{16}c)/(ft), \tag{16b}$$

where $f = A_{11}A_{22} - A_{12}^2$, for single ply k, $f^k = \bar{Q}^k_{11}\bar{Q}^k_{22} - (\bar{Q}^k_{12})^2$.

Taking a configuration of single ply, then Eqs. (16a) and (16b) become

$$E_{xx} = \frac{\sigma_{xx}}{\varepsilon_{xx}} = (\bar{Q}_{11}a^k - \bar{Q}_{12}b^k + \bar{Q}_{16}c^k)/a^k \tag{17a}$$

and

$$G_{x\theta} = \frac{\tau_{x\theta}}{\varepsilon_{x\theta}} = (\bar{Q}_{11}a^k - \bar{Q}_{12}b^k + \bar{Q}_{16}c^k)/f^k. \tag{17b}$$

To account for shear–normal coupling effect, the value of $\bar{Q}^k_{11}$ in Eq. (12) and the value of $G_{x\theta}$ in calculating C_s are replaced by E_{xx} and $G_{x\theta}$ obtained in Eqs. (16a) and (16b), respectively. For symmetric balanced laminate or orthotropic plies, the terms $\bar{Q}_{16}$ and $\bar{Q}_{26}$ vanish and Eqs. (16a) and (16b) can be re-written as

$$E_{xx} = \left(A_{11} - \frac{A_{12}^2}{A_{22}}\right)/t. \tag{18a}$$

Similarly $G_{x\theta}$ reduces to

$$G_{x\theta} = A_{66}/t. \tag{18b}$$

For single ply, Eqs. (18a) and (18b) become

$$E_{xx} = \left(\bar{Q}_{11}^{k} - \frac{(\bar{Q}_{12}^{k})^2}{\bar{Q}_{22}^{k}} \right) \tag{19a}$$

and

$$G_{x\theta} = \bar{Q}_{66}^{k}. \tag{19b}$$

Eqs. (18a) and (18b) are similar to that of Bauchau [2] and Singh and Gupta [5], used to evaluate equivalent modulus in EMBT. However, Eq. (19a) is similar to Eq. (13b) for updating the value of $\bar{Q}_{11}$ to account for Poisson's effect. It is to be noted that, in the present formulation, Poisson's effect is inherently included in the formulation of shear–normal coupling. This is clear by substituting ($\bar{Q}_{16} = \bar{Q}_{26} = 0$) for 0° and 90° ply angles in Eqs. (16a) and (16b) which reduce to Eqs. (13b) and (18a) and (18b).

2.3.3. Improvement to include bending–twisting coupling effect

In configurations at which $+\theta$ orientations are above the mid-plane there is an identical lamina (in the thickness and material) of $-\theta$ orientation at the same distance below the mid-plane (as shown in Fig. 2b), the bending–twisting coupling represented by the terms D_{16} and D_{26} (in the bending stiffness matrix [D]) for the laminate is zero. For symmetric laminate the terms D_{16} and D_{26} cannot be zero unless $\theta = 0^\circ$ or 90°. The bending–twisting stiffness coefficient [3] is given by

$$C_{BT} = \sum_{k=1}^{n} \bar{Q}_{16}^{(k)} \left[r_{o(k)}^4 - r_{i(k)}^4 \right]. \tag{20}$$

The expression for strain energy is modified as

$$U = \frac{1}{2} \int_0^l \left\{ C_B \left[\left(\frac{\partial \alpha}{\partial x} \right)^2 + \left(\frac{\partial \beta}{\partial x} \right)^2 \right] + C_S \left[\left(\frac{\partial w}{\partial x} - \alpha \right)^2 + \left(\frac{\partial v}{\partial x} - \beta \right)^2 \right] + \frac{C_{BT}}{2} \left[\left(\frac{\partial \phi}{\partial x} \right) \cdot \left(\frac{\partial \alpha}{\partial x} \right) + \left(\frac{\partial \phi}{\partial x} \right) \cdot \left(\frac{\partial \beta}{\partial x} \right) \right] + C_T \left(\frac{\partial \phi}{\partial x} \right)^2 \right\} \mathrm{d}x. \tag{21}$$

3. Layerwise beam theory

Several investigators (Singh and Gupta [5] and Gubran [9]) have used layerwise beam theory for the analysis of composite tubular shafts. This theory is obtained by reduction from the layerwise shell theory after imposing the condition of zero cross-section distortion. Referring to Fig. 3, the displacement field of shell theory modified to give rise to flexural modes only is given by

$$U_{zk} = \bar{u}_k(x) \cos\theta, \quad V_{zk} = -\bar{w}(x) \sin\theta, \quad W = \bar{w}(x) \cos\theta. \tag{22}$$

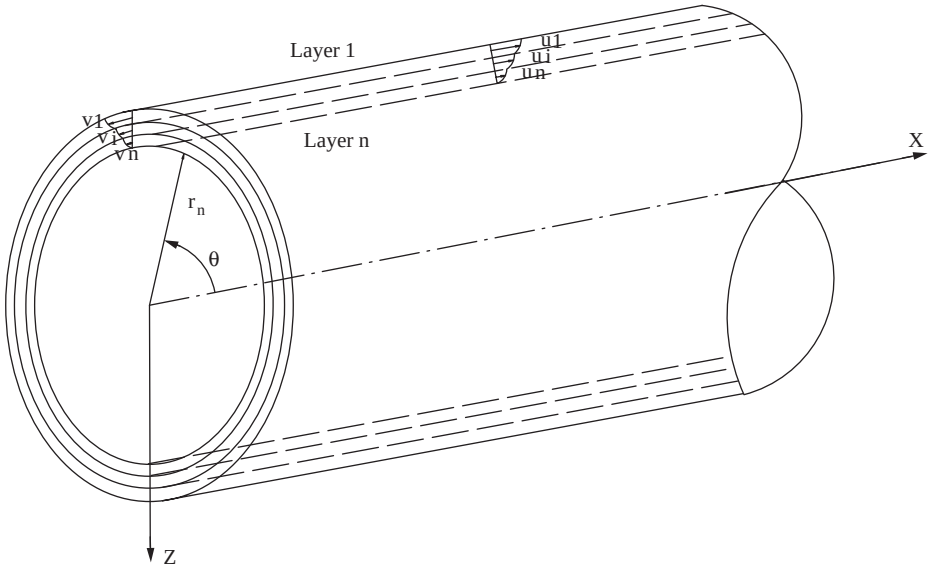

Fig. 3. Displacement field in layerwise beam theory.

The strain and kinetic energies can be expressed [5] as

$$U = \frac{\pi}{2}\sum_{k=1}^{n}\int_0^l \Bigg[\Big\{\Big(u_{k+1,x}^2 + u_{k,x}^2 + u_{k+1,x}u_{k,x}\Big)\frac{r_k t_k}{3} + \Big(u_{k+1,x}^2 - u_{k,x}^2\Big)/12\Big\}\bar{Q}_{11k} + \Bigg\{(u_{k+1}+u_k)^2\frac{a_k}{4} + \Big(u_{k+1}^2 - u_k^2\Big)\Big(1 + \frac{a_k r_k}{t_k}\Big) + (u_{k+1}-u_k)^2\big(a_k r_k^2 - r_k t_k\big)/t_k^2 + w_{,x}^2 r_k t_k + w_{,x}(u_{k+1}+u_k)t_k\Bigg\}\bar{Q}_{66k} + \Big\{w_{,x}^2 r_k t_k + \big(u_{k+1}^2 + u_k^2 - 2u_k u_{k+1}\big)r_k/t_k + 2\big(w_{,x}u_{k+1} - w_{,x}u_k\big)r_k t_k\Big\}\bar{Q}_{55k}\Bigg]\,\mathrm{d}x \tag{23}$$

where

$$a_k = \ln\left[\frac{(r_k + t_k/2)}{(r_k - t_k/2)}\right],$$

$$T = \frac{\pi}{2}\int_0^l \sum_{k=1}^{n}\rho_k\left[\frac{r_k t_k}{3}\big(\dot{u}_{k+1}^2 + \dot{u}_k^2 + \dot{u}_{k+1}\dot{u}_k\big) + 2\dot{w}^2 r_k t_k + \frac{t_k^2}{12}\big(\dot{u}_{k+1}^2 + \dot{u}_k^2\big)\right]\mathrm{d}x, \tag{24}$$

where $u_{zk}(x)$ and $w(x)$ are the amplitudes of u and w displacements in Cartesian coordinates which are expressed in series functions as

$$\bar{u}_{zk}(x) = \sum_{k=1}^{m} U^k f^k(x), \quad \bar{w}(x) = \sum_{k=1}^{m} W^k g^k(x). \tag{25}$$

On substituting Eq. (25) in the expressions of U and T and taking the variation of the total energy with respect to the unknown solution coefficients, a set of $(n+2)m$ equations are obtained which can be solved as a standard eigenvalue problem.

The values of longitudinal and shear stiffness $\bar{Q}_{11}$ and $\bar{Q}_{66}$ in Eq. (23) are updated to account for shear–normal coupling in a similar manner as that of modified EMBT and substituted for calculating the natural frequencies.

4. Results and discussion

A graphite/epoxy shaft simply supported on rigid bearings is considered. Shaft material properties are: longitudinal, transverse and shear modulii of 130, 10 and 7 GPa, respectively. Poisson's ratio and density are 0.25 and 1500 kg/m^3. Shaft geometrical parameters are: length 1 m, mean diameter 100 mm and a total thickness of 4 mm. To study the effects of stacking sequence and different coupling mechanisms on shaft natural frequencies, several cases have been considered. Both formulations of modified EMBT and LBT have been used. Natural frequencies obtained from both theories have been compared and studied in detail.

4.1. Comparison between modified EMBT and LBT excluding different coupling effects

To study the validation of formulation and programming, the results obtained from modified EMBT are compared with that of the LBT [5]. In order to have a basis for comparison, Poisson's and other coupling effects are ignored. Results presented in Table 1, clearly show excellent agreement of the natural frequencies obtained from both theories for shafts with single ply of fibre angle varying from 0° to 90°. As expected, natural frequencies in the first three modes are found to decrease with the value of fibre angle increasing from 0° to 90°. The shaft studied by Zinberg and Symmonds [1] is also analysed using the two theories. As it is clear from Table 2, the fundamental natural frequency obtained from the present work using modified EMBT (i.e. 5552 rev/min) is very close to the value of 5555 rev/min obtained by the present work using LBT [5] with $G_{13} = G_{23} = 0$.

Table 1
Comparison of natural frequencies (Hz) excluding Poisson's and different coupling effects

Ply angle (°)	LBT			Modified EMBT		
	1st	2nd	3rd	1st	2nd	3rd
0	428.04	1227.72	2056.44	427.85	1226.63	2052.49
15	442.50	1432.92	2576.95	442.40	1434.94	2574.00
30	390.52	1410.59	2787.43	390.49	1410.65	2785.92
45	292.75	1105.74	2297.63	292.74	1105.58	2297.00
60	199.99	767.66	1627.53	199.98	767.59	1627.27
75	150.77	577.09	1219.06	150.77	577.04	1218.84
90	140.57	528.59	1092.06	140.56	528.50	1092.18

Table 2
Comparison of critical speed as obtained by different investigators using different formulations with that obtained using modified EMBT

Investigator	Critical speed (rev/min)	Method of determination
Zinberg and Symmonds [1] (theoretical)	5780	Equivalent modulus beam theory
Zinberg and Symmonds [1] (experimental)	5500	Forced vibration response for the shaft supported on rolling element bearing conditions but under non-rotating conditions
Henrique dos Reis et al. [10]	4950	FEM, with beam elements derived from Donnell's shell theory
Singh and Gupta [5]	5746	Equivalent modulus beam theory, simple support function
	5747	Equivalent modulus beam theory, flexible supported function with high support stiffness (0.17×10^{12} N/m) as used by Henrique dos Reis et al. [10].
Singh and Gupta [5]	5332	LBT (with $G_{13} = G_{23} = 0$)
	5617	LBT (with $G_{13} = 6.9$ GPa, $G_{23} = 0$),
	5620	LBT (with $G_{13} = G_{23} = 6.9$ GPa),
Kim and Bert [4]	5872	Sanders shell theory
	6399	Donnell shallow shell theory
Bert [3]	5919	Bernoulli–Euler beam theory
Bert and Kim [4]	5788	Bresse–Timoshenko beam theory
Chen and Peng [6]	5714	Timoshenko beam theory and finite element method
Present work	5332	Modified equivalent beam theory (including Poisson's effect)
	5552	Modified equivalent beam theory (without including Poisson's effect)
Present work, using LBT (Singh and Gupta [5])	5555	LBT (without including Poisson's effect, with $G_{13} = G_{23} = 0$)
	5817	LBT (without including Poisson's effect, with $G_{13} = 6.9$ GPa, $G_{23} = 0$)
	5820	LBT (without including Poisson's effect, with $G_{13} = G_{23} = 6.9$ GPa)

Rotor properties: $L = 2.47$ m, mean radius $= 0.0635$ m, $t = 0.1321 \times 10^{-3}$ m, 10 layers of equal thickness from inner most $(90^\circ, 45^\circ, -45^\circ, [0^\circ]_6, 90^\circ)$; $\rho = 1965$ kg/m^3; $E_{11} = 211$ GPa, $E_{22} = 24.1$ GPa, $G_{12} = 6.9$ GPa, $v_{12} = 0.36$

4.2. Comparison between modified EMBT and LBT theories including Poisson's effect only

The effect of Poisson's coupling on shaft natural frequencies is studied in the case of a shaft made of single ply of 4 mm thickness. Both the modified EMBT and LBT are used for calculating

shaft natural frequencies. As explained earlier, Poisson's coupling effect is incorporated by replacing $\bar{Q}_{11}^{k}$ in Eq. (3) by $\bar{Q}_{11m}^{k}$ as defined in Eq. (13b). Effects of shear–normal and bending–twisting coupling are excluded. Results obtained are presented in Table 3. These clearly show very good agreement between the natural frequencies as obtained from modified EMBT and LBT for the first three modes of shafts with different ply angles. Comparison of results of Tables 1 and 3 shows that Poisson's coupling gives rise to a reduction in the shaft natural frequencies. The amount of reduction is dependent on the shaft ply angle. Table 4 gives the amount of reduction in the first mode as calculated by LBT. It is minimum for 0° and 90° ply angles and has a maximum value at 45° ply angle. The maximum reduction in the natural frequency of the first mode (as obtained by LBT as shown in Table 4) is about 26% (i.e from 292.7 to 216.7 Hz) for 45° ply angle. The fundamental natural frequency of Zinberg and Symmonds [1] shaft is also calculated. As shown in Table 2, natural frequencies obtained from present analysis (5332 rev/min) agree well with that of Singh and Gupta [5] using LBT with ($G_{13} = G_{23} = 0$) and taking Poisson's effect into account. It also shows a close agreement with the value (5500 rev/min) obtained experimentally by Zinberg and Symmonds [1] and to that obtained by Henrique dos Reis et al. [10]. Both the modified EMBT and LBT are used to calculate the natural frequency of the same shaft excluding Poisson's effect. The results obtained, for this case with $G_{13} = G_{23} = 0$, by both theories are in close agreement. Layerwise beam theory excluding Poisson's effect, for a shaft with $G_{13} = G_{23} =$ 6.9 GPa, gives a slightly less value (by 0.9%) for the first mode natural frequency (5820 Hz) than that predicted by Bert and Kim [4] using Sander shell theory (5872 Hz). It is also slightly higher (by about 0.5%) compared to that predicted by Bert and Kim [4] using Bresse–Timoshenko beam theory (5788 Hz). It is also observed that including Poisson's effect reduces the natural frequency from 5552 to 5332 Hz (i.e. by about 4%) as in the case of modified EMBT, and from 5555 to

Table 3
Comparison of natural frequencies (Hz) including Poisson's effects only

Ply angle (°)	LBT			Modified EMBT		
	1st	2nd	3rd	1st	2nd	3rd
0	427.328	1226.653	2055.427	427.135	1225.237	2051.499
15	430.316	1405.966	2544.83	430.221	1405.054	2542.049
30	325.367	1204.32	2443.779	325.347	1204.064	2442.807
45	216.786	833.341	1769.57	216.781	833.176	1769.302
60	165.300	639.131	1367.839	165.297	639.094	1367.689
75	145.906	559.376	1184.081	145.902	559.326	1183.878
90	140.240	527.461	1090.432	140.234	527.379	1090.106

Table 4
Percentage reduction in the first mode due to Poisson's effect as calculated by LBT

Ply angle (°)	0	15	30	45	60	75	90
% reduction	0.164	2.754	16.684	25.947	17.345	3.226	0.227

5332 Hz in the case of LBT with $G_{13} = G_{23} = 0$. Similarly, for the case $G_{13} = G_{23} = 6.9$ GPa, there is a reduction in the natural frequency from 5820 to 5620 Hz (i.e. by about 3.5%).

4.3. Effect of stacking sequence

To study the effect of stacking sequence on shaft natural frequencies, a shaft with four plies scheme was considered with two plies of 0° and 90° ply angles. The natural frequencies have been calculated for different combinations. Poisson's effect is taken into account; however, other coupling effects of shear–normal and bending–twisting are excluded. It is well known that the longitudinal modulus is maximum for 0° ply angle and minimum for 90° ply angle. For this reason, different locations of 0°and 90° ply angles give rise to different shaft natural frequencies. Singh and Gupta [5] have reported that EMBT does not differentiate between the stacking sequences; it considers the laminate so thin that the effect of all layers is assumed to act at the mean radius. However, in the present modified EMBT, the effect of the stacking sequence is taken into account while calculating the equivalent longitudinal and inplane shear modulii. Results presented in Table 5 show that the natural frequencies as obtained by both theories are different for different stacking sequences of 0° and 90° ply angles. As expected, it is maximum for configurations in which 0° ply angle is placed at the outermost position and minimum for configurations in which 0° ply is placed at the innermost position. From the results obtained by modified EMBT, it is clear that the first mode natural frequency varies in the range from 331.5 to 345.5 Hz (4.5%). Similarly the second and third mode natural frequencies vary in the ranges 1055.6–1084 Hz (2.5%), and 1876.3–1907.9 Hz (1.5%), respectively. The results obtained by EMBT [5] show the same values of 339, 1071 and 1895 Hz for the first, second and third modes, respectively for all stacking sequences. However, the modified EMBT has taken into account the effect of different stacking sequences similar to that of LBT. This is clear from the close agreement of the results obtained from both theories for different configurations. In a similar study, the effect of placing different ply angles at different positions along the shaft thickness on the natural frequency is studied. Two plies of 0° and 45° ply angles were taken, as it is well known that 0° ply angle has a longitudinal modulus much larger than that of 45° ply angle. Accordingly, the bending

Table 5
Variation of natural frequencies (Hz) with stacking sequence

Configuration	LBT			Modified EMBT		
	1st	2nd	3rd	1st	2nd	3rd
90,90,0,0	346.735	1093.655	1931.904	345.508	1083.983	1907.939
0,0,90,90	330.444	1047.112	1855.032	331.500	1055.628	1876.276
0,90,90,0	338.925	1071.792	1896.808	338.787	1070.539	1893.051
90,0,0,90	338.548	1070.329	1893.407	338.507	1069.973	1892.419
0,90,0,90	334.630	1059.275	1875.537	335.110	1063.059	1884.671
90,0,90,0	342.775	1082.544	1913.962	342.112	1077.228	1900.487
45,45,45,0	319.837	1188.506	2422.782	319.565	1185.038	2409.689
0,45,45,45	305.028	1134.293	2313.571	305.28	1137.543	2325.98

natural frequencies are controlled by the position of 0° ply angle rather than 45° ply angle. It is expected that as 0° ply angle moves towards the outer radius, the natural frequencies will increase. Table 5 presents the effect of relative positions of 0° and 45° ply angles on the shaft natural frequencies. It is observed that first mode natural frequency increases from 305 to 319 Hz as 0° ply angle is moved from the innermost to outermost position. An increase of the order 5% is observed in the second and third mode natural frequencies also. This is clear from the results obtained by modified EMBT and LBT. However, EMBT gives the same value of 313, 1165 and 2375 Hz for first, second and third modes, respectively for both configurations.

4.4. Effect of shear–normal coupling

In the present analysis shear–normal coupling effect is accounted for by taking the contribution of the terms $\bar{Q}_{16}$ and $\bar{Q}_{26}$ in the calculation of longitudinal and inplane shear modulii in both of modified EMBT and LBT. The effect of bending–twisting coupling is not included here. Generally, for a laminate of configurations having $+\theta$ in one side from the mid-plane and $-\theta$ (of the same thickness and material) on the other side of the mid-plane, the coupling terms $\bar{Q}_{16}$ and $\bar{Q}_{26}$ are automatically cancelled and shear–normal coupling is not present. Examination of Eq. (16b) which accounts for updating the value of $\bar{Q}_{11}$ to be substituted in the calculations of longitudinal modulus shows that Poisson's effect is inherently accounted for. This is clear by putting $\bar{Q}_{16}$ and $\bar{Q}_{26} = 0$, which reduces Eq. (16a) to Eq. (13b) which accounts for Poisson's effect only. Table 6 shows the effect of shear–normal coupling on the natural frequencies of the shaft considered earlier, but made of single ply of total thickness of 4 mm. Results obtained from modified EMBT and LBT are in excellent agreement. These also show that there is a significant reduction in the shaft natural frequencies obtained by including shear–normal coupling effect. However, the amount of reduction is different for different ply angles which indicates that shear–normal coupling depends strongly on the fibre angle. Observations made from Table 6 show that for 0° and 90° ply angle, shear–normal coupling is not present and the natural frequencies are the same as that obtained by accounting for Poisson's effect only (as shown in Table 3). However, for other ply angles there is a considerable reduction in the natural frequencies. The maximum reduction in the first mode is about 30% (i.e. from 325.4 to 226.9 Hz)

Table 6
Variation of the natural frequencies (Hz) including shear–normal coupling effect

Ply angle (°)	LBT			Modified EMBT		
	1st	2nd	3rd	1st	2nd	3rd
0	427.328	1226.653	2055.427	427.135	1225.237	2051.499
15	326.468	1055.622	1896.457	326.391	1054.897	1894.269
30	226.898	813.504	1595.378	226.875	813.240	1594.441
45	177.790	661.52	1350.92	177.778	661.497	1350.355
60	154.100	579.373	1197.217	154.093	579.282	1196.850
75	143.332	539.377	1115.778	143.325	539.293	1115.449
90	140.240	527.461	1090.432	140.234	527.378	1090.106

corresponding to 30° ply angle. The variation of shear–normal coupling is associated with the variations of the coupling terms $\bar{Q}_{16}$ and $\bar{Q}_{26}$ with different ply angles. It is maximum at 30° ply angle and absent at 0° and 90° ply angles. This explains the maximum reduction in the natural frequency obtained at 30° ply angle. The decrease in the second and third modes natural frequencies due to the presence of shear–normal effect is also substantial, i.e. 1024.3–813.2 Hz, and 2442.8–1594.4 Hz, respectively, for 30° ply angle.

4.5. Effect of bending–twisting coupling

Bending–twisting coupling is a phenomenon associated with composite structures. This gives significantly different results as compared to cases in which this coupling is exactly zero. However, if the number of plies in the structure is increased, the effect of bending–twisting coupling will be small and can be neglected. In the present work, EMBT is modified to account for bending–twisting effect. The strain energy associated with bending–twisting is added to the total strain energy of the shaft. Initially, a shaft of similar geometrical and material properties to that analysed by Bert and Kim [4] is studied. Later, this work has been extended to account for Poisson's effect. The shaft material properties as given by Bert and Kim [4] are: longitudinal and transverse modulii of 139 GPa, 11 GPa, shear modulii $G_{12} = G_{13}$ and G_{23} are 6.05 GPa and 3.78 GPa. Poisson's ratio and density are 0.313 and 1578 kg/m^3 respectively. Shaft geometrical parameters are length 2.47 m, mean diameter 126.9 mm and total thickness of 1.321 mm.

Results as obtained by the present work using modified EMBT taking into account bending–twisting coupling effect only (all other coupling effects are excluded) are compared with that of Bert and Kim [4]. Table 7 (columns 3 and 5) gives a comparison for the first mode natural frequency obtained by Bert and Kim [4] and the present work using modified EMBT. Bending–twisting coupling effect is taken in both formulations. Analyses of the results show a close agreement in the natural frequencies for different configurations as obtained by both formulations. It also shows the reduction in the natural frequencies for shafts with different ply angles due to bending–twisting coupling effect. This reduction is maximum, 14.35% (i.e. from 82.2–70.3 Hz), as shown in Table 8 for 30° ply angle. No reduction is observed for 0° and 90° ply angles. This is expected for such ply angles which have no coupling terms, i.e. $\bar{Q}_{16}$and $\bar{Q}_{26} = 0$ and consequently D_{16} and D_{26} are also absent.

4.6. Effects of combined shear–normal and bending–twisting coupling

Further, the previous study of Bert and Kim [4] shaft has been extended to include Poisson's effect only and combined effects of Poisson's and bending–twisting coupling. Results for these cases are presented in columns 6 and 7 of Table 7. Comparison of the results presented in column 6 obtained by including Poisson's effect only and that of column 5 obtained by including bending–twisting only shows that Poisson's effect causes greater reduction in the shaft natural frequency as compared to that obtained by bending–twisting coupling effect. Also, the amount of reduction in the natural frequency is maximum at 45° ply angle, while for bending–twisting coupling, it is maximum at 30° ply angle. The variation in the reduction of shaft natural frequency due to Poisson's effect and bending–twisting coupling can be explained as follows. Reduction in the natural frequency due to Poisson's effect is mainly due to variation of the coupling term $\bar{Q}_{12}$

Table 7
Variation of first mode natural frequency (Hz) with different coupling effects

Ply angle (°)	Bert and Kim [4]		Present work		Present work			
					Poisson's effect included		Shear–normal included	
	Bending Twisting excluded	Bending Twisting included	Bending Twisting excluded	Bending Twisting included	Bending Twisting excluded	Bending Twisting included	Bending Twisting excluded	Bending Twisting included
(1)	(2)	(3)	(4)	(5)	(6)	(7)	(8)	(9)
0	101.2	101.2	101.33	101.33	100.99	100.99	100.99	100.99
15	96.47	86.82	96.56	86.87	93.06	82.78	69.03	52.86
30	81.67	69.95	82.16	70.3	65.48	48.98	41.56	10.49
45	60.4	52.38	61.1	52.83	41.77	27.89	35.9	17.77
60	41.07	37.97	41.57	38.32	32.84	28.56	31.96	27.55
75	31.53	31.23	31.91	31.53	30.63	30.23	30.57	30.17
90	30.05	30.05	30.38	30.38	30.27	30.27	30.27	30.27

Table 8
Percentage reduction in the first mode due to different coupling effects

Ply angle (°)	0	15	30	45	60	75	90
% reduction due to BT only (cols. 4&5 of Table 7)*	0	10.0	14.3	13.3	7.5	0.9	0
% reduction due to Poisson's only (cols. 4&6 of Table 7)*	0.34	3.6	20.3	31.6	21.0	4.0	0.36
% reduction due to SN only (cols. 6&8 of Table 7)*	0	25.8	36.5	14.0	2.6	0.2	0
% reduction due to combined effect (cols. 4&9 of Table 7)*	0.34	45.2	87.2	70.9	33.7	5.4	0.36

*The percentage decrease at any column is calculated based on the values given in Table 7.

which is maximum at 45° ply angle. However, the reduction in the natural frequency due to bending–twisting coupling effect is mainly due to the coupling term $\bar{Q}_{16}$ which is maximum at about 30° ply angle. Later, this study has been extended (using modified EMBT) to take into account, first, shear–normal coupling effect only, and second, all coupling effects in combination. Results are presented in columns 8 and 9 of Table 7, respectively. The reduction in the natural frequency due to shear–normal coupling is more than that due to bending–twisting coupling and Poisson's effect. This is also maximum at 30° ply angle which is mainly due to the variation of the coupling term $\bar{Q}_{16}$. A drastic reduction in the shaft natural frequency for different ply angles is obtained by including all coupling effects in combinations as shown in column 9 of Tables 7 and 8. For example, for 30° ply angle, the fundamental natural frequency drops down to 10.49 Hz from a value of 81.67 Hz, when both the bending–twisting and shear–normal coupling effects are taken. Effects of different coupling mechanisms on shaft first natural frequency for different ply angles are shown in Fig. 4. It is observed that different couplings give rise to different amounts of reduction in the natural frequency for shafts with different ply angles. At 0° and 90° ply angles, no reduction is observed in the natural frequency due to bending–twisting coupling; however,

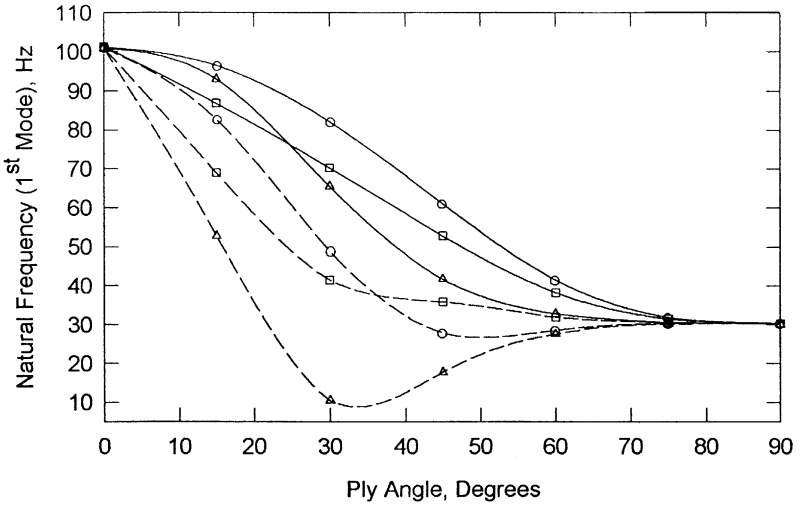

Fig. 4. Variation of natural frequency with different ply angles due to different coupling mechanisms. —○—, excluding all coupling; —□—, with bending–twisting (only); —△—, with Poisson's effect (only); --○--, with Poisson's effect and bending–twisting; --□--, with shear–normal (only); --Δ--, including all coupling.

Poisson's effect is minimum. At ply angles in the range 70–90°, coupling effects either taken individually or in combination are small. It is also clear from Fig. 4, that the amount of reduction in the natural frequency due to bending–twisting coupling is more than that due to Poisson's effect for ply angles in the range 5–27°. However, for ply angles in the range 27–85°, Poisson's effect is more dominant than that of bending–twisting coupling. This is mainly due to variation of the coupling terms ($\bar{Q}_{12}$, $\bar{Q}_{16}$ and $\bar{Q}_{26}$) with the ply angle. Similarly the amount of reduction in the natural frequency due to shear–normal coupling is more than that due to the combined effect of Poisson and bending–twisting for shafts with ply angles in the range 0–35°. However, for shafts with ply angles in the range of 35–90°, the combined effect of Poisson and bending–twisting is more than that due to shear–normal coupling. A significant amount of reduction in the shaft natural frequency is obtained due to combined effect at ply angles in the range of 30–35°.

5. Conclusion

In this paper, EMBT with transverse shear deformation, rotary inertia and gyroscope effects has been modified. The modifications take into account plies stacking sequence and different coupling mechanism effects. Shear–normal coupling effect also has been included in the LBT. Results obtained from both theories have been compared with each other and with that available in the literature. The following are the main points which can be drawn from the results of this study:

1. In spite of its simplicity, the natural frequencies obtained using modified EMBT excluding different coupling effects agree well with those obtained using LBT and with that reported in

the literature. Effects of stacking sequence and unsymmetric configuration, which are the main disadvantages of EMBT, have been incorporated and the results obtained compared well with that of LBT.

2. Different coupling mechanisms, as obtained from both theories, were found to reduce shaft natural frequencies. The percentage reduction depends on coupling mechanisms available in different ply angles. For Poisson's effect the maximum reduction in the shaft natural frequency is found to be at about 45° ply angle, however for shear–normal and bending–twisting coupling, the maximum reduction is found to be at about 30° ply angle.
3. Analysis has shown that, Poisson's effect will be inherently incorporated in the formulation of shear–normal coupling. For balanced configuration shear–normal effect is not present, but Poisson's effect will be present and has to be incorporated.

References

[1] H. Zinberg, M.F. Symmonds, The development of an advanced composite tail rotor driveshaft, *Presented at 26th Annual National Forum of American Helicopter Society*, Washington, DC, 1970, pp. 1–14.

[2] O.A. Bauchau, Optimal design of high speed rotating graphite/epoxy shafts, *Journal of Composite Materials* 17 (1983) 170–181.

[3] C.W. Bert, The effect of bending–twisting coupling on the critical speed of a driveshaft, *Proceedings Sixth Japan–US Conference on Composite Materials*, Orlando, FL, Techonomic, Lancaster, PA, 1993, pp. 29–36.

[4] C.W. Bert, C.K. Kim, Whirling of composite material driveshafts including bending–twisting coupling and transverse shear deformation, *Journal of Vibration and Acoustics* 117 (1) (1995) 7–21.

[5] S.P. Singh, K. Gupta, Composite shaft rotordynamic analysis using a layerwise theory, *Journal of Sound and Vibration* 191 (5) (1996) 739–756.

[6] L.-W. Chen, W.-K. Peng, Dynamic stability of rotating composite shaft under periodical axial compressive loads, *Journal of Sound and Vibration* 212 (2) (1998) 215–230.

[7] L.-W. Chen, W.-K. Peng, The stability behavior of rotating composite shaft under axial compressive loads, *Composite Structures* 41 (1998) 253–263.

[8] H.B.H. Gubran, S.P. Singh, K. Gupta, Stresses in composite shafts subjected to unbalance excitation and transmitted torque, *International Journal of Rotating Machinery* 6 (4) (2000) 235–244.

[9] H.B.H. Gubran, Dynamic Stress Analysis and Optimization Studies on Fibre-Reinforced Composite Shafts, PhD Thesis, IIT, Delhi, 2000.

[10] L.M. Henrique Dos Reis, R.B. Goldman, P.H. Verstrate, Thin walled laminated composite cylinderical tubes–part III: Critical speed analysis, *Journal of Composites Technology and Research* 9 (2) (1987) 58–62.